HHS Public Access

Author manuscript

Hepatology. Author manuscript; available in PMC 2021 May 01.

Published in final edited form as:

Hepatology. 2020 May ; 71(5): 1813–1830. doi:10.1002/hep.30928.

Hepatocyte Stress Increases Expression of YAP and TAZ in Hepatocytes to Promote Parenchymal Inflammation and Fibrosis

Meghan Mooring[1], **Brendan H. Fowl**[2], **Shelly Z.C. Lum**[2], **Ye Liu**[1], **Kangning Yao**[1], **Samir Softic, M.D.**[2,3], **Rory Kirchner**[4], **Aaron Bernstein**[5], **Aatur D. Singhi, M.D., Ph.D.**[6], **Daniel G. Jay, Ph.D.**[5], **C. Ronald Kahn, M.D.**[3], **Fernando D. Camargo, Ph.D.**[7,8], **Dean Yimlamai, M.D., Ph.D.**[1,2,6]

[1]Division of Gastroenterology and Nutrition, Department of Pediatrics, Children's Hospital of Pittsburgh of UPMC, Pittsburgh, PA 15224;

[2]Division of Gastroenterology and Nutrition, Department of Pediatrics, Boston Children's Hospital, Boston, MA 02115;

[3]Section on Integrative Physiology and Metabolism, Joslin Diabetes Center and Department of Medicine, Harvard Medical School, Boston, MA 02115;

[4]Department of Biostatistics, Harvard T.H. Chan School of Public Health, Boston, MA 02115;

[5]Department of Developmental, Molecular, and Chemical Biology, School of Medicine, Tufts University, Boston, MA 02111;

[6]Pittsburgh Liver Research Center, University of Pittsburgh/University of Pittsburgh Medical Center, Pittsburgh, PA 15261;

[7]The Stem Cell Program, Boston Children's Hospital, Boston, MA 02115;

[8]Department of Stem Cell and Regenerative Biology, Harvard University, Cambridge, MA 02138.

Abstract

Activated hepatocytes are hypothesized to be a major source of signals that drive cirrhosis, but the biochemical pathways that convert hepatocytes into such a state are unclear. We examined the role of the Hippo pathway transcriptional coactivators, YAP/TAZ in hepatocytes to facilitate cell-cell interactions that stimulate liver inflammation and fibrosis. Using a variety of genetic, metabolic and liver injury models in mice, we manipulated Hippo signaling in hepatocytes and examined its effects in non-parenchymal cells to promote liver inflammation and fibrosis. YAP expressing hepatocytes rapidly and potently activate the expression of proteins that promote fibrosis (COL1A1, TIMP1, PDGFc, TGFβ2) and inflammation (TNF, IL1β). They stimulate expansion of myofibroblasts and immune cells followed by aggressive liver fibrosis. In contrast, hepatocyte-specific YAP and YAP/TAZ knockouts exhibit limited myofibroblast expansion, less

Correspondence to: dean.yimlamai@chp.edu.

Author Contribution: MM and DY designed the experiments and wrote the manuscript. BHF, SZCL, YL and KY performed experiments. SS and CRK analyzed genetic models associated with IGFR/IR. AB performed cell migration assays. RK performed bioinformatic analysis. ADS curated and analyzed patient liver samples. All authors provided intellectual input, vetted and approved the final manuscript.

Conflict of Interest Statement: The authors declare no conflict of interest.

inflammation, and decreased fibrosis after carbon tetrachloride injury despite a similar degree of necrosis as controls. We identified CYR61 as a chemokine that is upregulated by hepatocytes during liver injury but is expressed at significantly lower levels in mice with hepatocyte-specific deletion of YAP or TAZ. Gain and loss of function experiments with CYR61 *in vivo* point to it being a key chemokine controlling liver fibrosis and inflammation in the context of YAP/TAZ. There is a direct correlation between levels of YAP/TAZ and CYR61 in liver tissues of high-grade NASH patients.

Conclusion—Liver injury in mice and humans increases levels of YAP/TAZ/CYR61 in hepatocytes, thus attracting macrophages to the liver to promote inflammation and fibrosis.

Keywords

liver regeneration; signal transduction; transcriptional regulation; immune response

INTRODUCTION

An estimated 3.9 million American adults have chronic liver disease with liver failure being among the top five causes of adult death in the United States(1) and the United Kingdom(2). Worldwide, approximately 50 million people are affected by chronic liver disease with an estimated 1.3 million people dying of liver disease in 2015(3). While there are diverse causes of chronic liver disease, long-term liver stress and injury likely lead to pathologic remodeling along common biochemical pathways. Understanding the contribution of these pathways to liver disease is a first step to developing therapies that may span a wide variety of conditions.

Hepatocytes form the metabolic and detoxifying workhorse of the liver. They are one of the first cells to encounter small molecules and infectious particles absorbed across the intestine and because of this, they are subjected to tremendous biochemical stresses. There is an emerging consensus that such stress leads to the dedifferentiation of hepatocytes and is a major source of liver cancer(4). Hepatocyte death is thought to elicit the release of signaling molecules, leading to liver inflammation and myofibroblast activation(5, 6). This can lead to liver fibrosis and eventually, cirrhosis. Some investigators have suggested that secretion of inflammatory signals can also occur from activated hepatocytes(7, 8), but the underlying mechanism(s) that switch hepatocytes into such a state remain unclear.

There has been great interest in the Hippo signaling pathway because it is a critical regulator of liver size(9) and is an important tumor suppressor pathway that is mutated in a number of human cancers including HCC(10, 11). The Hippo pathway tightly regulates the proteins YAP/TAZ, transcriptional co-activators that act as a gatekeepers controlling proliferation and growth(9). YAP consistently is enriched in liver disease including non-alcoholic steatohepatitis (NASH)(12), biliary atresia(13), and primary sclerosing cholangitis(14). The signals that cause YAP to be elevated as well as the consequence of this enrichment is a matter of debate. In addition, YAP is consistently enriched in multiple cell types within diseased tissue. The precise role(s) that YAP plays likely differ depending on the cell type during the evolution of liver disease.

Previously, we defined that the Hippo signaling pathway is a critical determinant maintaining hepatocyte fate in the liver(15). We primarily focused on the role of hepatocyte Hippo signaling in controlling a stem cell-like fate, but in that study, we often noted that other cell types were rapidly recruited and proliferated in response to our hepatocyte-specific manipulations. From these observations, we hypothesize that there are non-cell autonomous effects of hepatocyte YAP levels, which influence the local microenvironment leading to chronic inflammation, cirrhosis and cancer.

Here, we demonstrate that hepatocyte levels of YAP and/or TAZ are directly related to the degree of liver inflammation and fibrosis and the macrophage chemoattractant Cyr61 is consistently responsive to YAP/TAZ levels across multiple scenarios. Cyr61 loss in the context of YAP overexpression results in a marked reduction in liver weight, macrophage proportion, and myofibroblast expansion. Cyr61 is a key Hippo Pathway target downstream of YAP/TAZ(16), acting as one of the earliest inflammatory signals after hepatocyte injury.

MATERIALS AND METHODS

Murine Lines

Tetracycline-inducible YAP S127A(TetOYap)(17), conditional YAP floxed(18), conditional TAZ floxed(19), conditional insulin receptor/insulin-like growth factor 1 receptor mice(20) were used in this study. Conditional reverse tetracycline activator, tdTomato and EYFP mice were obtained from the Jackson Laboratories(Bar Harbor, ME). CYR61-EGFP reporter mice were obtained from The GENSAT Project(www.gensat.org). Experiments were performed beginning at eight to twelve weeks of age. Male and female mice were used in the YAP inducible portion of the study. Models using various forms of injury(CCl_4, CDE, IR/IGFR) were analyzed using only male mice. A minimum of three mice were examined for each displayed result. All mouse procedures and protocols were approved by an AAALAC-accredited facility.

Adeno-associated Viral(AAV) Gene Delivery, YAP Overexpression, Macrophage Depletion, Cyr61 Expression, Cas9-mediated Cyr61 Deletion

AAV-TBG-LacZ(AAV-LacZ, Cat# AV-8-PV0142) or AAV-TBG-Cre(AAV-Cre, Cat# AV-8-PV1091) were purchased from the University of Pennsylvania Vector Core. The indicated genotypes were infected through retro-orbital injections of 10^{11} pfu/mouse to achieve infection of >99% of hepatocytes or 10^8 pfu/mouse in the case of clonal analysis. YAP expression is induced in TetOYAP animals 3 days after AAV-Cre delivery by providing doxycycline(1 mg/ml) *ad libitum* in their drinking water. In order to deplete monocytes/macrophages from TetOYAP mice, a 200 μl intravenous injection of either PBS or clodronate liposomes(Encapsula Nanoscience, Cat# NC0302518) were given to mice the day prior to doxycycline administration. Injections were repeated every three days until sacrifice.

To exogenously express Cyr61, human Cyr61 replaced EGFP in AAV-TBG-EGFP (Addgene.org,Cat# 105535). This vector was packaged by Vector Biolabs(Malvern, PA) and

injected at a concentration of 3.5×10^{11} per mouse. AAV-TBG-EGFP was delivered at equal concentrations as controls.

To perform *in vivo* deletion of hepatocyte Cyr61, a pair of single guide RNAs(sgRNA) targeting Cyr61 were designed(sgCyr61–1: CTTCTCCACTTGACCAGACTG, sgCyr61–3: CTCAGCCCTGCGACCACACCA) and cloned into pX602-AAV-TBG-saCas9(Addgene.org, Cat# 61593). AAV was co-injected into TetOYAP mice at equimolar concentrations to AAV-TBG-Cre. Control virus(Vector Biolabs, Cat# 7131) with AAV-TBG-Cre was delivered to TetOYAP mice as controls. YAP expression was induced as above.

Additional methods are found in the Supplemental Methods.

RESULTS

Increased Hepatocyte YAP Activity Leads to Rapid αSMA$^+$ Myofibroblast Activation, Inflammation and Fibrosis

We examined how varying intracellular hepatocytic YAP levels affects their interactions with the microenvironment by utilizing a previously described method of inducible hepatocyte-specific YAP expression(15). This system combines intravenous delivery of a hepatocyte-specific Cre-recombinase(AAV-Cre) into mice containing inducible alleles for tetracycline-inducible expression of YAP S127A, a constitutive-active form of YAP(TetOYAP)(17) and a reverse tetracycline-controlled transactivator(rtTA) (Figure S1A). One week after doxycycline administration, αSMA$^+$ myofibroblasts emerged from the portal area and continued to expand in the ensuing weeks (Figure 1A, αSMA). Collagen deposition was first seen around the portal tracts two weeks after TetOYAP induction (YAP-Tg) and continued to aggressively expand outward from the portal areas of YAP-Tg livers, dominating more than 70% of the liver parenchyma at 6 weeks (Figure 1A, Collagen, Figure S1B).

We then examined the relationship of hepatocytes expressing YAP with αSMA$^+$ myofibroblasts by tracing EYFP expression after AAV-Cre infection. By staining for EYFP/αSMA and panCK/αSMA, we could identify that the Yap-Tg cells were distinct from αSMA$^+$ myofibroblasts. In comparison, αSMA$^+$ myofibroblasts displayed considerable overlap with Desmin$^+$ cells, suggesting that a large proportion are hepatic stellate cells (Figure 1B).

Inflammation is commonly associated with the development of liver fibrosis(21, 22), so we studied if there was an increase in immune cells in the liver shortly after YAP-Tg, but prior to the development of fibrosis. By immunohistochemistry(IHC), there was a profound increase in monocytes as identified by F4/80$^+$ two weeks after doxycycline administration (Figure 1C). One week after YAP-Tg, flow cytometry identified a nearly 3-fold increase in the proportion of liver neutrophils (6.5% vs 20.9%, n=8, $p<0.001$) and macrophages (8.9% vs 25.9%, n=10, $p<0.001$) in YAP-Tg as compared to control mice (Figure 1D).

Because of the increased myofibroblast activity and the rapid expansion of immune cells in YAP-Tg livers prior to the visible deposition of collagen, we assessed if there was an

accumulation of proinflammatory/profibrotic signals. We confirmed YAP-Tg activity five days after doxycycline administration by examining a number of reported Hippo target genes (Figure S1C). In particular, the Hippo target and profibrotic ligand CTGF could be easily detected by qPCR as well as by RNA in situ hybridization(RISH) throughout the liver parenchyma (Figure S1D). In these mice, there was a gradual increase in markers of fibrosis by qPCR at 4 weeks. Additionally, as YAP levels increased, there was an enrichment of ligands associated with inflammation and fibrosis, with a concomitant decrease in the anti-inflammatory cytokine, IL-10, which persisted over time (Figure S1E).

In order to assess the contribution of inflammation to the development of fibrosis, we targeted monocytes/macrophages for depletion because they have been previously implicated in the development of liver fibrosis(23, 24). Yap-Tg mice given clodronate liposomes reduced liver monocytes/macrophages by 99% ($p<0.001$) over control Yap-Tg mice. In parallel Col1a1 (87%, $p<0.04$) and TIMP1 (94%, $p<0.02$) were reduced (Figure 1E). Less αSMA activation was present in Yap-Tg/clodronate mice (Figure 1F/G) as well as a concomitant reduction in fibrosis (Figure 1G).

Next, we titrated AAV-Cre delivery to observe clonal behavior and better understand how YAP-Tg cells interact with their microenvironment *in situ*. Clonal analysis demonstrated that YAP-Tg cells are tightly associated with αSMA^+ and $F4/80^+$ cells at 4 and 8 weeks (Figure 2A, Figure S2A). Others have suggested that YAP overexpression can stimulate epithelial to mesenchymal transition (EMT) (25, 26), which could contribute to fibrosis. At 4 and 8 weeks, YAP-Tg cells showed 1% and 0.5% of EYFP/αSMA^+ cells, respectively (Figure S2A). $Sox9^+$ cells co-expressed SMA^+ at 2% and 1% at 4 and 8 weeks, respectively (Figure S2B). We examined RNA microarray data from sorted YAP-Tg cells at 1 and 6 weeks after induction (15). It confirmed our prior report of strong and increasing expression of ductal markers in YAP-Tg cells (Figure S2C), but with respect to EMT, we found no significant change in fibroblast markers over time (Figure S2D).

YAP-Tg cells were also enriched in mRNA transcripts of secreted ligands by RISH (Figure 2B). We confirmed that YAP-Tg cells could be a source of secreted cyto/chemokines by comparing purified populations of normal hepatocytes and YAP-Tg expressing cells (Figure 2C). Two weeks of YAP-Tg expression did not significantly affect the expression of several hepatocyte associated genes (Figure S2E) but did potently affect the expression of several known Hippo target genes (Figure 2D). These YAP-Tg cells express high levels of several secreted genes associated with fibrosis (TGFβ2, PDGFc) and inflammation (IL-1β, TNFα, Figure 2E). These data suggest that hepatocytes that upregulate YAP become a source of secreted signals to recruit and activate myofibroblasts and immune cells.

Chronic Liver Injury Leads to Elevated YAP/TAZ Activity

We examined several mouse models of chronic liver injury to define the degree and effect physiologic injury leads to elevated hepatocytic YAP and TAZ levels. Chronic carbon tetrachloride (CCl_4) administration results in broad increase in YAP and TAZ expression throughout the liver parenchyma via IHC (Figure 3A) as well as Western blotting (Figure 3B). We assessed if YAP expression is associated with EMT upon CCl_4 injury. At baseline, no YAP/αSMA^+ cells were found (Figure S3A). In acute and chronic injury, YAP/αSMA^+

cells increased to 3% (1x CCl_4, n=1215) and 2% (7x CCl_4, n=1376), respectively (Figure S3A). We also assessed panCK/αSMA$^+$ at the indicated timepoints, finding 0%, 0% and 3.7% panCK/αSMA$^+$ at 0, 1x and 7x CCl_4 (Figure S3B).

Then, we examined the choline-deficient ethionine (CDE) supplemented diet model, which mimics alcoholic liver disease. CDE diet demonstrated clear enrichment of YAP in hepatocytes (Figure 3C). YAP and TAZ expression appeared maximal seven days after introduction of the diet with a modest reduction by 14 days, albeit still elevated over baseline (Figure 3D). Finally, we examined a previously described metabolic model of lipodystrophy that results in livers with the characteristics of non-alcoholic steatohepatitis (NASH). In this model, floxed alleles of the insulin receptor (IR) and insulin-like growth factor-1 receptor (IGFR) are removed in adipocytes resulting in defective lipid uptake. These mice display several metabolic features of NASH including hyperglycemia, hyperlipidemia and hyperinsulinism(20). These mice have severe bridging fibrosis with an associated elevation in hepatocyte YAP levels (Figure 3E). We confirmed by Western blotting broad increases in YAP and TAZ (Figure 3F), and that several target genes of the Hippo pathway were elevated in their livers (Figure 3G). Under multiple forms of toxic and metabolic injury, increased hepatocyte levels and activity of YAP/TAZ are associated with the development of liver inflammation and fibrosis.

Reduction in Hepatocyte YAP/TAZ Levels Attenuates Liver Inflammation and Fibrosis.

In order to determine the contribution of hepatocyte YAP/TAZ activity to liver remodeling during chronic injury, we generated mice with hepatocyte-specific deletion of *Yap fl/fl* (YKO) or *Yap/Taz fl/fl* (DKO) with AAV-Cre followed by CCl_4 treatment. Hepatocyte-specific deletion of YAP and/or TAZ was verified by immunostaining (Figure 4A) and immunoblotting (Figure 4B). As controls, we delivered AAV-LacZ to homozygous *Yap fl/fl* mice (Control) and treated them in a similar fashion to experimental mice.

YAP/TAZ overexpression during regeneration is well known to drive anti-apoptotic and proliferative gene programs (27, 28), therefore loss of these molecules, particularly in the context of injury and regeneration, should lead to reduced proliferation. Using 5-ethynyl-2'-deoxyuridine (EdU) incorporation as a proxy for cell division, we did not a detect a difference in the rate of proliferation between control and YKO livers during homeostasis (Data not shown). In contrast, hepatocyte proliferation was reduced by 67% in YKO mice after CCl_4 injury ($p<0.01$, Figure 4C).

Cellular injury and death results in the release of damage-associated molecular patterns (DAMPs) which activate myofibroblasts and immune cells, leading to inflammation and fibrosis(29). In CCl_4 treated YKO livers, there was a modest, but insignificant increase in necrosis (Figure S4A, 14% vs 10.6%) and alanine aminotransferase (ALT) levels (Figure S3B, 790 vs 596). However, we observed that YKO and DKO mice had 50% and 58% less collagen deposition than controls, respectively ($p<0.001$). YKO and DKO were not significantly different from each other (Figure 5A). αSMA$^+$ myofibroblasts were reduced in YKO and DKO as compared to controls with αSMA$^+$ myofibroblasts consistently accumulating around the central venous areas. The typical bridging phenotype for αSMA$^+$ myofibroblasts was not evident in the YKO or DKO groups (Figure 5B).

Several studies have implicated liver inflammation, particularly macrophage infiltration, as a strong contributor to the development of liver fibrosis(23, 24), therefore we examined if inflammation was affected in the livers of YKO and DKO models of chronic CCl_4 treatment. Immunostaining demonstrated an overall reduction in liver monocytes of YKO and DKO genotypes as compared to controls (Figure 5C). We confirmed by flow cytometry that this primarily was from a reduced percentage of macrophages in YKO mouse livers as compared to controls (Figure 5D, 20.2% vs. 12.7%). The percentage of liver neutrophils showed no difference as compared to controls (Figure S3C, 25% vs 28.1%). This data suggests that activated hepatocytes secrete signals through YAP/TAZ, which direct the activity of immune and myofibroblasts to remodel the liver after chronic injury.

Hepatocyte gene expression programs define Liver Regeneration and Extracellular Remodeling

In order to distinguish gene programs and, ultimately, the individual gene targets that could be responsible for the inflammatory and fibrotic phenotypes involved with hepatocyte-specific YAP and YAP/TAZ knockouts, we generated RNA-seq libraries from the hepatocytes of uninjured control, DKO, chronic CCl_4-treated control and DKO mice(Figure 6A). Principal component analysis (PCA) defined the primary determinants of differences between samples as the presence of YAP/TAZ and/or their exposure to CCl_4(PC1, 50%; PC2, 15%). All samples showed a clear separation into their respective treatment conditions(Figure 6B). DKO/CCl_4 treated samples had the highest median per-gene TPM variance(0.616) while other hepatocyte treatments displayed a lower median per-gene TPM variance(0.123–0.193). We found 1749 genes that showed a $p<0.05$ and were at least two-fold differentially expressed between conditions (Figure 6C).

In hepatocytes, untreated DKO resulted in 287 differentially expressed genes (149 Upregulated, 138 Downregulated) compared to untreated control. Consistent with a known role for YAP/TAZ in mitotic spindle assembly, DNA checkpoint control, and cell fate determination(15, 30, 31), we found gene programs including *Mitotic Cytokinesis* (GO:0000281; NES = −2.17) to be downregulated and *Cell Fate Determination* (GO:0001709; NES = 1.8) to be upregulated (Figure 6D). CCl_4 injury in control animals demonstrated 289 upregulated and 75 downregulated genes compared to untreated control, a majority which were involved in phagocytosis (GO:0006911; NES = 2.2), extracellular matrix organization (GO:0030198; NES = 1.89) and leukocyte migration (GO:0002688; NES = 1.8; Figure S5A).

In comparing Ctl/CCl_4 injury to DKO/CCl_4 injury, there was a total of 1749 differentially expressed genes (1256 upregulated, 493 downregulated). YAP/TAZ are typically described as transcriptional coactivators, so in the context of injury it was unanticipated that their loss resulted in: 1) A larger number of upregulated genes in DKO/CCl_4 as compared to Ctl/CCl_4 and, 2) Of the genes shared by Ctl/CCl_4 and DKO/CCl_4, their expression is higher in the DKO/CCl_4 group (Figure 6C). We confirmed that DKO/CCl_4 injury results in higher levels of gene expression than Ctl/CCl_4 by comparing independent whole liver qPCR for Apoa4, Lcn2 and Lyz2 (Figure S5B).

DKO to DKO/CCl_4 demonstrated that the most differentially expressed gene programs to be a combination involved in immune cell migration and chromosome checkpoint regulation (Figure S5C). When comparing gene programs associated with Ctl/CCl_4 to DKO/CCl_4, we found metabolic programs to be more prominent in the DKO/CCl_4 scenario while immune migratory programs predominated in the Ctl/CCl_4 condition, specifically *Myeloid Leukocyte Migration* (GO:0097529; NES −2.5). This bioinformatic profiling is consistent with the finding of fewer monocytes in DKO/CCl_4 livers as compared to Ctl/CCl_4 (Figure 5C/D).

RNA-seq profiling of live hepatocytes revealed that under conditions of stress, such as in CCl_4 injury or loss of YAP/TAZ, hepatocytes actively participate in moderating liver inflammation and myofibroblast activation. Many of these injury response programs involve signaling through the Hippo pathway. We found YAP/TAZ plays a role in dampening and moderating the variability of gene expression in the context of CCl_4 injury. These data point to hepatocytes having a transcriptionally active response to injury, acting as a central coordinator for extracellular activities involved in liver regeneration.

Hepatocyte-derived Cyr61 is Primarily Regulated by the Hippo Pathway and is a Key Macrophage Chemoattractant in CCl_4 Liver Injury

From our RNA-seq hepatocyte profiling, we sought to identify chemokines which would be activated in response to CCl_4 injury and whose expression would be blunted in the context of YAP/TAZ knockout, similar to YAP and TAZ (Figure S6A). We examined chemokines previously described as Hippo Pathway target genes as well as pro-inflammatory genes we observed to be increased in the context of hepatocyte-specific YAP-Tg. After injury, these genes showed either low or significantly increased levels of expression despite the loss of YAP/TAZ (Figure S6B). This suggests that in this context, these genes either do not significantly contribute to the inflammatory/fibrotic phenotype induced by CCl_4 or are primarily regulated by other signaling pathways. The only cytokine found to satisfy the expression criteria outlined above was the glycoprotein Cyr61 (Figure 7A).

Using Cyr61-EGFP reporter mice, we examined the localization and expression of Cyr61 after CCl_4 injury. Hepatocytes in the central region, areas where inflammatory infiltrates are predominantly found had upregulated Cyr61 expression after CCl_4 injury (Figure 7B). Soluble Cyr61 increased the migration of the macrophage cell line, RAW264.7 by nearly two-fold using *in vitro* transwell assays (0.98 vs 1.93, $p<0.04$; Figure S7A). We then examined the consequence of hepatocyte-expressed Cyr61, independent of injury by infecting mice with hepatocyte-specific AAV-Cyr61. As compared to EGFP infected mice, the livers of AAV-Cyr61 mice upregulated SMA and F4/80 expression (Figure 7C). We confirmed that macrophages were enriched in Cyr61 livers over controls (0.6 vs 1.6%, $p<0.02$, Figure S7B) by flow cytometry.

We then examined if loss of Cyr61 could abrogate the inflammatory and fibrotic effect of induced YAP expression. We used CRISPR/Cas9 to genetically knock out Cyr61 in our inducible TetOYAP model (YAP-Tg/sgCyr61). We delivered hepatocyte specific AAV-saCas9 containing either control or Cyr61 sgRNAs along with AAV-Cre followed by doxycycline administration. YAP-Tg/sgCyr61 livers were 14% smaller than YAP-Tg after one week of TetOYAP induction (n=6/group; p=0.01) and 29% smaller than after two weeks

of induction (n=5/group; p=0.002). All YAP-Tg groups were consistently larger than control mice (Figure 7D). We confirmed YAP induction and Cyr61 deletion in the YAP-Tg/sgCyr61 groups by immunoblotting their livers (Figure 7E). Between YAP-Tg and YAP-Tg/sgCyr61 cohorts, we did not find a significant difference in proliferation (9.9/100 vs 6.9/100 $pH3^+$ nuclei) or YAP expression between the two (Figure S7C), indicating the observed difference in size is not a result of differential proliferation.

We then focused on the hypothesis that Cyr61 is a key macrophage chemoattractant of the Hippo pathway. YAP-Tg/sgCyr61 livers had fewer monocytes by immunohistochemistry than YAP-Tg livers(Figure 7F, F4/80), which we confirmed by flow cytometry (Figure 7G, 32.8% vs 20.7%, $p<0.05$), at two weeks after YAP induction. αSMA and F4/80 were diminished by immunoblotting (Figure 7E) and immunostaining(Figure 7F). There was also a significant reduction in fibrotic markers in YAP-Tg/sgCyr61 as compared to YAP-Tg at two weeks after YAP induction (Figure 7H).

Finally, to document a direct correlation in human patients between the degree of liver inflammation/fibrosis and YAP/TAZ/CYR61 expression, we examined the livers of a cohort of control and NASH patients. Patients were characterized as either control or NASH histology groups (n=10, each) by a clinical pathologist (Supplemental Table 1). Liver samples from these patients were immunostained for YAP and the hepatocyte marker HNF4α. Several fields of hepatocytes in both conditions were examined and scored for the frequency of nuclear YAP localization in $HNF4\alpha^+$ cells. Patients with NASH commonly displayed double positive nuclei than control patients (Figure 8A, 0.66 vs 0.13, $p<0.001$).

Immunostaining for YAP/TAZ consistently showed intense hepatocytic staining for these molecules, particularly enriched along areas of fibrosis/inflammation (Figure 8B). Performing RISH for CYR61 in these samples showed a strong direct correlation for both YAP/CYR61 (R^2 0.83, $p<0.001$) and TAZ/CYR61 (R^2 0.75, $p<0.001$). qPCR on these liver samples revealed TAZ/CYR61 to have a modest, significant correlation (Figure S8, R^2 0.49, $p<0.02$). This data strongly supports that hepatocyte signaling through the Hippo pathway effectors YAP/TAZ leads to the expression of key chemokines such as CYR61. Increased CYR61 expression stimulates and recruits liver macrophages which support the development of liver fibrosis.

DISCUSSION

In response to organ injury, there is a complex dance that cells orchestrate to result in functional regeneration. YAP/TAZ have a long established role in regulating cell proliferation and survival(17, 27, 32) and are increasingly being recognized to have other roles such as controlling cellular metabolism(33, 34). These primarily are cell autonomous activities, but proper organ regeneration also requires coordinating critical non-cell autonomous activities, including the removal of dead/dying cells, generation of new extracellular matrices and defining cell/organ polarity.

Here, we show that in chronic liver injury hepatocyte YAP/TAZ activity increases resulting in proliferation. In the context of YAP as well as YAP/TAZ deletion, there was a reduction in

macrophage recruitment, defective myofibroblast activation, and less fibrosis, despite similar degrees of necrosis. DAMPs released by cellular necrosis are proposed to be an important component of inflammatory/fibrotic signaling in chronic injury(5, 35), but in the context YAP/TAZ loss, there was less inflammation and fibrosis despite similar degrees of DAMP release. We examined the expression levels of known DAMPs such as HMGB1 in our YAP/TAZ knockout model and did not note significant expression differences (Data not shown). DAMP release from dying hepatocytes appears to stimulate a certain degree of inflammation/fibroblast activation, which we believe is supplemented by signals from other sources, such as YAP/TAZ activated cells.

Persistent YAP/TAZ activity causes hepatocytes to dedifferentiate into biliary cells (15, 36) with accumulating evidence that such a process occurs across many forms of chronic liver injury (37–39). In this study, we targeted hepatocytes prior to YAP/TAZ induction or liver injury, thus we are unable to distinguish the contribution of hepatocytes versus their transdifferentiated progeny to inflammation and fibrosis. As the phenotype and the activity with which they contribute to fibrosis likely differ, potential studies targeting YAP, TAZ, or CYR61 in preexisting liver disease can offer critical insights into their prospective utility and feasibility.

Furthermore, YAP/TAZ activity causes EMT(25, 26, 40) which potentially can drive collagen deposition. In response to persistent YAP expression in both YAP-Tg and CCl_4 injury models, a small number of cells appeared double positive for epithelial and fibroblast markers, although no differences in EMT gene expression were seen in isolated epithelial cells. Future studies will have to investigate if EMT is required for epithelial cells to promote fibrosis under stress.

Conflicting evidence exists for positive and negative roles for YAP/TAZ in regulating cellular immunity. Some studies suggest that YAP/TAZ antagonizes innate immune responses (41, 42), while in the context of cancer, epithelial YAP/TAZ activity leads to inflammation which is proposed to boost anti-tumoral responses(43) or promote tumor development(44). The context of YAP/TAZ activation is a key determinant of the signals that these activated hepatocytes secrete. In examining hepatocytes from a model of high consistent YAP levels (YAP-Tg), we validated the presence of ligands such as Ctgf, Ccl2(44) and TGFβ1(45), previously described fibrotic/inflammatory targets downstream of YAP/TAZ. In addition, we identified robust expression of other ligands strongly associated with inflammation and fibrosis (PDGFc, IL1β, TNFα). Conversely, liver injury where hepatocytic YAP/TAZ activation is more modest and brief, we were unable to identify the presence of these ligands despite a phenotype consistent with elevated YAP activity.

The only ligand that was consistently expressed in a pattern that could explain both scenarios was the glycoprotein Cyr61. Cyr61 is one of the most consistently reported Hippo pathway gene targets(16) and has been described as a macrophage chemoattractant in non-alcoholic steatohepatitis (46). Our experiments in manipulating Cyr61 expression in the context of increased YAP expression demonstrate that Cyr61 is one of the earliest and consistent Hippo targets to promote macrophage recruitment to areas of injury. Macrophage

number and phenotype are known contributors to liver fibrosis(23, 24) which likely account for the reduction in fibrosis in YAP and YAP/TAZ knockout mice.

Across multiple forms of liver injury, we identified an enrichment of hepatocytic YAP/TAZ suggesting that this is a common injury response. Our lipodystrophic mouse model, which mimics the lipotoxicity seen in NASH exhibits increases in YAP and TAZ. The disease severity in our cohort of NASH patients is directly related to hepatocytic YAP/TAZ/CYR61 levels. A recent study utilizing a diet induced model of NASH in mice reported that TAZ activation of IHH transcription is primarily responsible for the fibrotic remodeling in NASH(47). However, we found that a loss of YAP versus YAP/TAZ did not result in significant phenotypic differences after chronic injury. Overall, we propose that it is the total amount of cellular YAP/TAZ which determines the gene expression patterns that lead to inflammation and fibrosis.

Finally, the most surprising insight of this study involves how hepatocytes transcriptionally respond to injury in the absence of YAP/TAZ. Due to the perceived importance of YAP/TAZ as transcriptional coactivators, we predicted that fewer genes and less gene activation would occur in YAP/TAZ hepatocytes after injury. In contrast, we found a larger number, a higher magnitude of gene expression and greater variability in the absence of YAP/TAZ. A variety of mechanisms by which YAP/TAZ can moderate transcriptional activities have been described. These include direct transcriptional repression through TEAD(48), secondary repression through downstream microRNA targets(49), and direct association and sequestration of YAP with p72, a regulatory component of the microprocessor complex (50). Compared to control hepatocytes, DKO hepatocytes upregulated genes involved in metabolism to a higher degree after injury, which may be an inefficient use of scarce cellular resources during regeneration. Conversely, DKO hepatocytes did not activate genes associated with immune cell migration as efficiently as control hepatocytes, leading to less inflammation and fibrosis. Coupled with the higher variability in gene expression we identified, YAP/TAZ play a critical role in orchestrating proper gene activation during recovery.

YAP/TAZ are critical players in tissue regeneration, but their excessive activity can lead to pathologic remodeling. Therapeutic inhibition of a multifunctional molecule such as YAP/TAZ may lead to unwanted side-effects, so defining downstream YAP/TAZ targets such as Cyr61 is critical to advancing precision medicine. Here, we defined that Cyr61 loss ameliorates the inflammation and fibrosis from high YAP activity, while simultaneously preserving a tissues' proliferative capability.

Supplementary Material

Refer to Web version on PubMed Central for supplementary material.

Acknowledgments:

This work is supported by awards from Gilead Sciences (DY), the NIH K08 DK105351 (DY), K12 HD000850 (SS), NASPGHAN Foundation Young Investigator Award (SS), R01 DK099559 (FDC), R01 DK031036 (CRK), R01 DK033201 (CRK), R01 CA183119 (DGJ), the Harvard Digestive Disease Center to DY (2P30 DK034854) and Harvard Catalyst|The Harvard Clinical and Translational Science Center for bioinformatics support (UL1

RR025758). The content does not necessarily represent the official views of the National Center for Research Resources or the National Institutes of Health.

REFERENCES

1. Murphy SL, Xu J, Kochanek KD, Curtin SC, Arias E. Deaths: Final Data for 2015. Natl Vital Stat Rep 2017;66:1–75.
2. Patel V Deaths registered in England and Wales: 2016. In: Office for National Statistics; 2017 p. 1–13.
3. Organization WH. World Health Statistics 2017: Monitoring Health for the SDGs, Sustainable Development Goals. In: World Health Organization; 2017.
4. Sia D, Villanueva A, Friedman SL, Llovet JM. Liver Cancer Cell of Origin, Molecular Class, and Effects on Patient Prognosis. Gastroenterology 2017;152:745–761. [PubMed: 28043904]
5. Luedde T, Kaplowitz N, Schwabe RF. Cell death and cell death responses in liver disease: mechanisms and clinical relevance. Gastroenterology 2014;147:765–783 e764. [PubMed: 25046161]
6. Brenner C, Galluzzi L, Kepp O, Kroemer G. Decoding cell death signals in liver inflammation. J Hepatol 2013;59:583–594. [PubMed: 23567086]
7. He G, Karin M. NF-kappaB and STAT3 - key players in liver inflammation and cancer. Cell Res 2011;21:159–168. [PubMed: 21187858]
8. Marra F, Tacke F. Roles for chemokines in liver disease. Gastroenterology 2014;147:577–594 e571. [PubMed: 25066692]
9. Patel SH, Camargo FD, Yimlamai D. Hippo Signaling in the Liver Regulates Organ Size, Cell Fate, and Carcinogenesis. Gastroenterology 2017;152:533–545. [PubMed: 28003097]
10. Harvey KF, Zhang X, Thomas DM. The Hippo pathway and human cancer. Nat Rev Cancer 2013;13:246–257. [PubMed: 23467301]
11. Yu FX, Zhao B, Guan KL. Hippo Pathway in Organ Size Control, Tissue Homeostasis, and Cancer. Cell 2015;163:811–828. [PubMed: 26544935]
12. Machado MV, Michelotti GA, Pereira TA, Xie G, Premont R, Cortez-Pinto H, Diehl AM. Accumulation of duct cells with activated YAP parallels fibrosis progression in non-alcoholic fatty liver disease. J Hepatol 2015;63:962–970. [PubMed: 26070409]
13. Gurda GT, Zhu Q, Bai H, Pan D, Schwarz KB, Anders RA. The use of Yes-associated protein expression in the diagnosis of persistent neonatal cholestatic liver disease. Hum Pathol 2014;45:1057–1064. [PubMed: 24746211]
14. Bai H, Zhang N, Xu Y, Chen Q, Khan M, Potter JJ, Nayar SK, et al. Yes-associated protein regulates the hepatic response after bile duct ligation. Hepatology 2012;56:1097–1107. [PubMed: 22886419]
15. Yimlamai D, Christodoulou C, Galli GG, Yanger K, Pepe-Mooney B, Gurung B, Shrestha K, et al. Hippo Pathway Activity Influences Liver Cell Fate. Cell 2014;157:1324–1338. [PubMed: 24906150]
16. Lai D, Ho KC, Hao Y, Yang X. Taxol resistance in breast cancer cells is mediated by the hippo pathway component TAZ and its downstream transcriptional targets Cyr61 and CTGF. Cancer Res 2011;71:2728–2738. [PubMed: 21349946]
17. Camargo FD, Gokhale S, Johnnidis JB, Fu D, Bell GW, Jaenisch R, Brummelkamp TR. YAP1 increases organ size and expands undifferentiated progenitor cells. Current Biology 2007;17:2054–2060. [PubMed: 17980593]
18. Schlegelmilch K, Mohseni M, Kirak O, Pruszak J, Rodriguez JR, Zhou D, Kreger BT, et al. Yap1 acts downstream of alpha-catenin to control epidermal proliferation. Cell 2011;144:782–795. [PubMed: 21376238]
19. Xin M, Kim Y, Sutherland LB, Murakami M, Qi X, McAnally J, Porrello ER, et al. Hippo pathway effector Yap promotes cardiac regeneration. Proc Natl Acad Sci U S A 2013;110:13839–13844. [PubMed: 23918388]

20. Softic S, Boucher J, Solheim MH, Fujisaka S, Haering MF, Homan EP, Winnay J, et al. Lipodystrophy Due to Adipose Tissue-Specific Insulin Receptor Knockout Results in Progressive NAFLD. Diabetes 2016;65:2187–2200. [PubMed: 27207510]
21. Seki E, Schwabe RF. Hepatic inflammation and fibrosis: functional links and key pathways. Hepatology 2015;61:1066–1079. [PubMed: 25066777]
22. Pellicoro A, Ramachandran P, Iredale JP, Fallowfield JA. Liver fibrosis and repair: immune regulation of wound healing in a solid organ. Nat Rev Immunol 2014;14:181–194. [PubMed: 24566915]
23. Duffield JS, Forbes SJ, Constandinou CM, Clay S, Partolina M, Vuthoori S, Wu S, et al. Selective depletion of macrophages reveals distinct, opposing roles during liver injury and repair. J Clin Invest 2005;115:56–65. [PubMed: 15630444]
24. Karlmark KR, Weiskirchen R, Zimmermann HW, Gassler N, Ginhoux F, Weber C, Merad M, et al. Hepatic recruitment of the inflammatory Gr1+ monocyte subset upon liver injury promotes hepatic fibrosis. Hepatology 2009;50:261–274. [PubMed: 19554540]
25. Zhao B, Ye X, Yu J, Li L, Li W, Li S, Yu J, et al. TEAD mediates YAP-dependent gene induction and growth control. Genes & Development 2008;22:1962–1971.
26. Overholtzer M, Zhang J, Smolen GA, Muir B, Li W, Sgroi DC, Deng CX, et al. Transforming properties of YAP, a candidate oncogene on the chromosome 11q22 amplicon. Proc Natl Acad Sci U S A 2006;103:12405–12410. [PubMed: 16894141]
27. Zhao B, Wei X, Li W, Udan R, Yang Q. Inactivation of YAP oncoprotein by the Hippo pathway is involved in cell contact inhibition and tissue growth control. Genes & development 2007;21:2747–2761. [PubMed: 17974916]
28. Oka T, Mazack V, Sudol M. Mst2 and Lats kinases regulate apoptotic function of Yes kinase-associated protein (YAP). J Biol Chem 2008;283:27534–27546. [PubMed: 18640976]
29. Kubes P, Mehal WZ. Sterile inflammation in the liver. Gastroenterology 2012;143:1158–1172. [PubMed: 22982943]
30. Bolgioni AF, Ganem NJ. The interplay between centrosomes and the Hippo tumor suppressor pathway. Chromosome Res 2016;24:93–104. [PubMed: 26582635]
31. Weiler SME, Pinna F, Wolf T, Lutz T, Geldiyev A, Sticht C, Knaub M, et al. Induction of Chromosome Instability by Activation of Yes-Associated Protein and Forkhead Box M1 in Liver Cancer. Gastroenterology 2017;152:2037–2051 e2022. [PubMed: 28249813]
32. Dong J, Feldmann G, Huang J, Wu S, Zhang N, Comerford SA, Gayyed MF, et al. Elucidation of a universal size-control mechanism in Drosophila and mammals. Cell 2007;130:1120–1133. [PubMed: 17889654]
33. Cox AG, Hwang KL, Brown KK, Evason KJ, Beltz S, Tsomides A, O'Connor K, et al. Yap reprograms glutamine metabolism to increase nucleotide biosynthesis and enable liver growth. Nat Cell Biol 2016;18:886–896. [PubMed: 27428308]
34. Jeong SH, Kim HB, Kim MC, Lee JM, Lee JH, Kim JH, Kim JW, et al. Hippo-mediated suppression of IRS2/AKT signaling prevents hepatic steatosis and liver cancer. J Clin Invest 2018;128:1010–1025. [PubMed: 29400692]
35. Friedman SL, Sheppard D, Duffield JS, Violette S. Therapy for fibrotic diseases: nearing the starting line. Sci Transl Med 2013;5:167sr161.
36. Yovchev M, Jaber FL, Lu Z, Patel S, Locker J, Rogler LE, Murray JW, et al. Experimental Model for Successful Liver Cell Therapy by Lenti TTR-YapERT2 Transduced Hepatocytes with Tamoxifen Control of Yap Subcellular Location. Sci Rep 2016;6:19275. [PubMed: 26763940]
37. Lu WY, Bird TG, Boulter L, Tsuchiya A, Cole AM, Hay T, Guest RV, et al. Hepatic progenitor cells of biliary origin with liver repopulation capacity. Nat Cell Biol 2015;17:971–983. [PubMed: 26192438]
38. Tarlow BD, Pelz C, Naugler WE, Wakefield L, Wilson EM, Finegold MJ, Grompe M. Bipotential adult liver progenitors are derived from chronically injured mature hepatocytes. Cell Stem Cell 2014;15:605–618. [PubMed: 25312494]
39. Yanger K, Zong Y, Maggs LR, Shapira SN, Maddipati R, Aiello NM, Thung SN, et al. Robust cellular reprogramming occurs spontaneously during liver regeneration. Genes Dev 2013;27:719–724. [PubMed: 23520387]

40. Lei Q-Y, Zhang H, Zhao B, Zha Z-Y, Bai F, Pei X-H, Zhao S, et al. TAZ Promotes Cell Proliferation and Epithelial-Mesenchymal Transition and Is Inhibited by the Hippo Pathway. In: Molecular and Cellular Biology; 2008 p. 2426–2436. [PubMed: 18227151]

41. Wang S, Xie F, Chu F, Zhang Z, Yang B, Dai T, Gao L, et al. YAP antagonizes innate antiviral immunity and is targeted for lysosomal degradation through IKKvarepsilon-mediated phosphorylation. Nat Immunol 2017;18:733–743. [PubMed: 28481329]

42. Zhang Q, Meng F, Chen S, Plouffe SW, Wu S, Liu S, Li X, et al. Hippo signalling governs cytosolic nucleic acid sensing through YAP/TAZ-mediated TBK1 blockade. Nat Cell Biol 2017;19:362–374. [PubMed: 28346439]

43. Moroishi T, Hayashi T, Pan WW, Fujita Y, Holt MV, Qin J, Carson DA, et al. The Hippo Pathway Kinases LATS1/2 Suppress Cancer Immunity. Cell 2016;167:1525–1539 e1517. [PubMed: 27912060]

44. Kim W, Khan SK, Liu Y, Xu R, Park O, He Y, Cha B, et al. Hepatic Hippo signaling inhibits protumoural microenvironment to suppress hepatocellular carcinoma. Gut 2017;67:1692–1703. [PubMed: 28866620]

45. Lee DH, Park JO, Kim TS, Kim SK, Kim TH, Kim MC, Park GS, et al. LATS-YAP/TAZ controls lineage specification by regulating TGFbeta signaling and Hnf4alpha expression during liver development. Nat Commun 2016;7:11961. [PubMed: 27358050]

46. Bian Z, Peng Y, You Z, Wang Q, Miao Q, Liu Y, Han X, et al. CCN1 expression in hepatocytes contributes to macrophage infiltration in nonalcoholic fatty liver disease in mice. J Lipid Res 2013;54:44–54. [PubMed: 23071295]

47. Wang X, Zheng Z, Caviglia JM, Corey KE, Herfel TM, Cai B, Masia R, et al. Hepatocyte TAZ/WWTR1 Promotes Inflammation and Fibrosis in Nonalcoholic Steatohepatitis. Cell Metab 2016;24:848–862. [PubMed: 28068223]

48. Kim M, Kim T, Johnson RL, Lim DS. Transcriptional co-repressor function of the hippo pathway transducers YAP and TAZ. Cell Rep 2015;11:270–282. [PubMed: 25843714]

49. Tumaneng K, Schlegelmilch K, Russell RC, Yimlamai D, Basnet H, Mahadevan N, Fitamant J, et al. YAP mediates crosstalk between the Hippo and PI(3)K-TOR pathways by suppressing PTEN via miR-29. Nat Cell Biol 2012;14:1322–1329. [PubMed: 23143395]

50. Mori M, Triboulet R, Mohseni M, Schlegelmilch K, Shrestha K, Camargo FD, Gregory RI. Hippo signaling regulates microprocessor and links cell-density-dependent miRNA biogenesis to cancer. Cell 2014;156:893–906. [PubMed: 24581491]

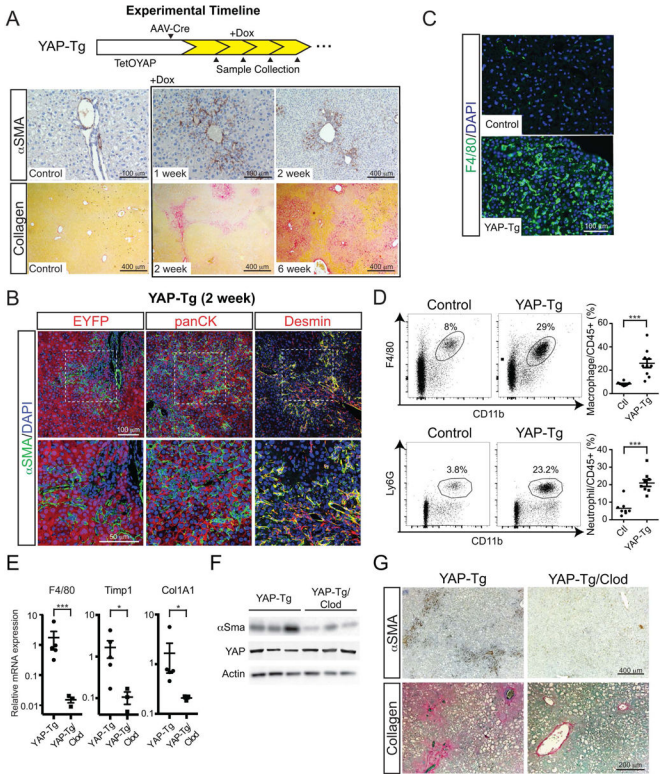

FIGURE 1. Hepatocyte-specific YAP expression activates αSMA$^+$ myofibroblasts and recruits immune cells resulting in liver fibrosis

A. Timeline of AAV-Cre delivery to adult TetOYAP mice, induction of YAP-Tg expression and subsequent sample collection. Representative α-smooth muscle actin (αSMA) and collagen staining from livers of TetOYAP mice at the indicated timepoints after doxycycline administration.

B. Confocal immunofluorescent liver staining of YAP-Tg mice after 2 weeks for the indicated proteins. Boxed area in upper picture is enlarged in the image below.

C. Immunofluorescent F4/80 liver staining of Control and YAP-Tg mice after 2 weeks.

D. Representative flow cytometry of liver neutrophils (CD45$^+$CD11b$^+$Ly6G$^+$) and macrophages (CD45$^+$CD11b$^+$Ly6G$^-$F4/80$^+$) one week after YAP-Tg induction. Percentages are of the gated population. Right, dot plots of all flow cytometry experiments (n=8, control; n=9, YAP-Tg).

E. Dot plots of whole liver RT-qPCR of the noted genes after YAP-Tg or YAP-Tg mice treated with clodronate (YAP-Tg/Clod) two weeks after induction. Horizontal line represents the mean, each dot represents an experiment. Error bars indicate standard error. *p<0.05, **p<0.01, ***p<0.001.

F. Immunoblots of the indicated proteins in YAP-Tg or YAP-Tg/Clod two weeks after induction.

G. Representative αSMA and collagen stain of YAP-Tg and YAP-Tg/Clod two weeks after YAP-Tg induction.

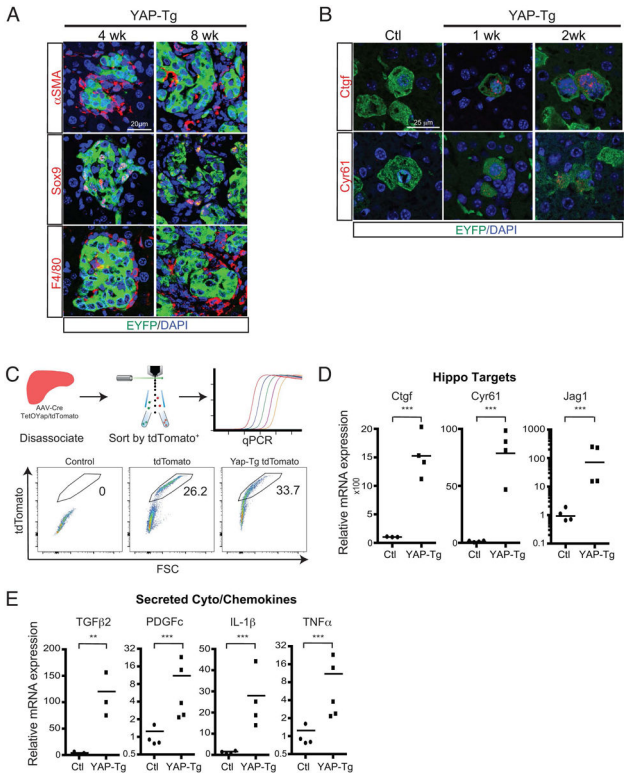

FIGURE 2. Clonal YAP-Tg Cells Intimately Interact with Myofibroblasts and Immune Cells

A. Immunofluorescent staining of either αSMA, Sox9, or F4/80 in clonal YAP-Tg populations after 4 and 8 weeks. EYFP labels YAP-Tg cells if doxycycline is administered.

B. Clonal analysis of control versus YAP-Tg cells after various time points for Ctgf and Cyr61 using RISH. EYFP labels YAP-Tg cells if doxycycline is administered.

C. Diagram/representative flow cytometry plots of strategy to isolate hepatocytes by tdTomato^{+} gene expression

D. qPCR dot plots of Hippo pathway target genes from sorted tdTomato^{+} hepatocytes.

E. qPCR dot plots of cyto/chemokines from control (Ctl) and YAP-Tg hepatocytes after 2 weeks of YAP-Tg expression. **p<0.01 ***p<0.001. Horizontal line represents the mean, each dot represents an experiment.

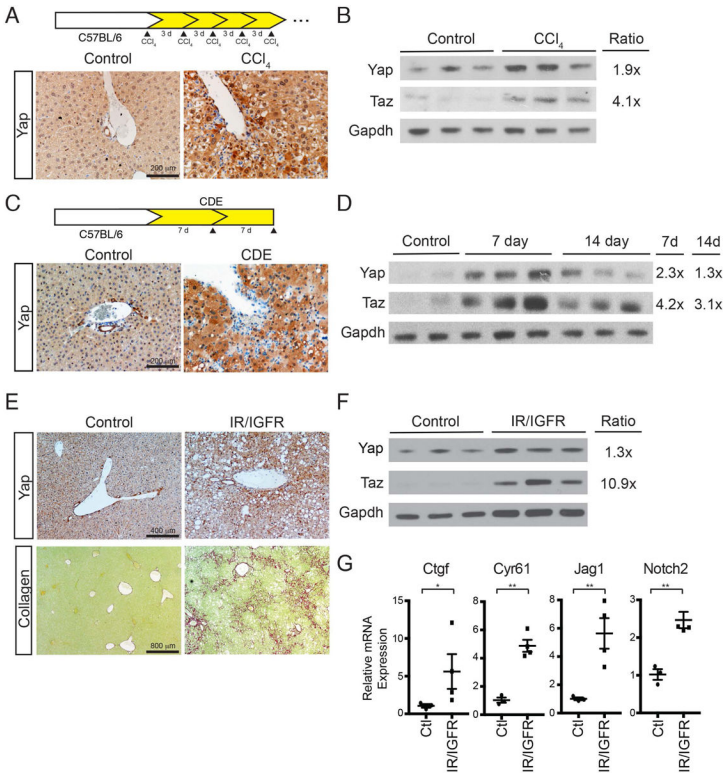

FIGURE 3. Multiple Forms of Toxic/Metabolic Liver Injury Lead to Increases in YAP/TAZ

A. Chronic CCl_4 treatment diagram and IHC for YAP expression after chronic CCl_4 treatment.

B. Whole liver immunoblot of YAP and TAZ after chronic CCl_4 treatment.

C. CDE diet administration diagram and IHC for YAP expression after one week treatment.

D. Whole liver immunoblot of YAP, and TAZ after CDE treatment for 7 and 14 days.

E. IHC for YAP expression in Adiponectin-Cre IR/IGFR mice and littermate controls at 12 months of age. Associated picrosirius red staining is seen below each IHC staining.

F. Whole liver YAP/TAZ immunoblots of IR/IGFR mice.

G. Dot plots of whole liver qRT-PCR of littermate control and IR/IGFR mice at 12 months (n=3, each).

For immunoblots, Ratio indicates relative enrichment of indicated protein after normalization to GAPDH. *p<0.05, **p<0.01. Error bars indicate standard error of the mean.

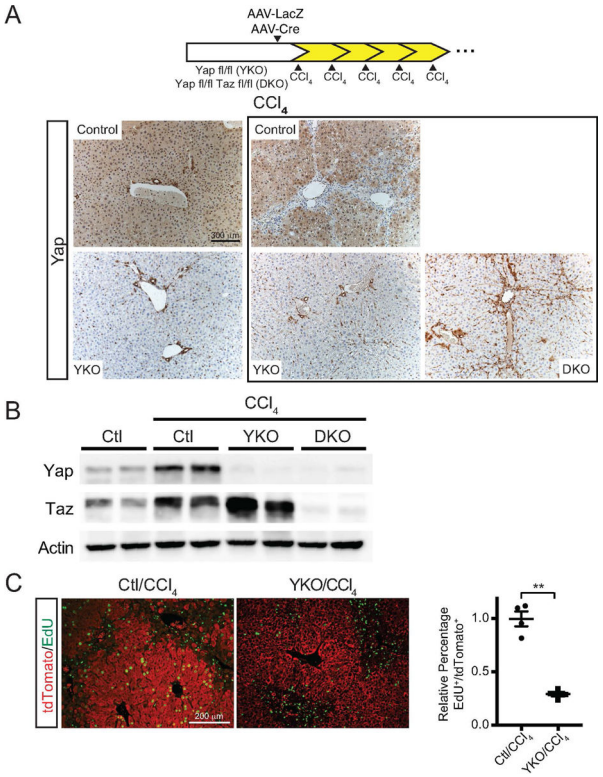

FIGURE 4. YAP and TAZ are Predominantly Found within Hepatocytes of the Liver

A. Experimental design of *Yap fl/fl*(YKO) or *Yap/Taz fl/fl*(DKO) hepatocyte knockout and chronic CCl_4 treatment. Controls-YKO mice given AAV-LacZ. Representative YAP IHC of the indicated treatments. Box indicates chronic CCl_4 treatment.

B. Whole liver immunoblot of YAP, TAZ, and GAPDH after the indicated chronic CCl_4 treatments.

C. Representative tdTomato (Red) and EdU (Green) staining in Control and YKO mice subjected to a single dose of CCl_4. Dot plot to the right indicates the relative number of EdU^+ cells per $tdTomato^+$ population for each treatment (n=4, each). **p<0.01. Error bars indicate standard error of the mean.

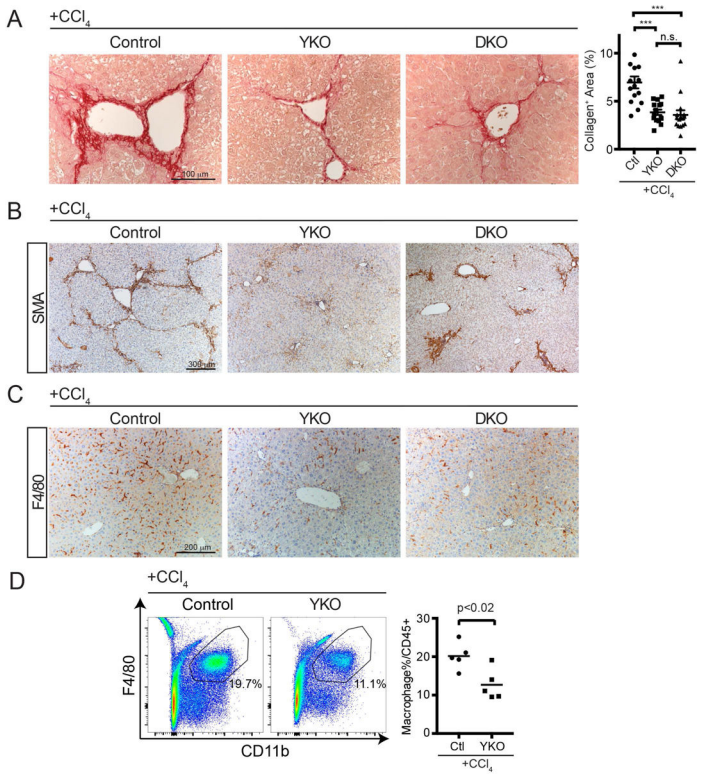

FIGURE 5. Loss of Hepatocyte YAP or YAP/TAZ attenuates Liver Fibrosis after CCl_4 Injury

A. Representative Picro-Sirius Red staining of mice from the indicated genotypes after chronic CCl_4 treatment. Dot plot to the right indicates quantification of collagen staining per unit area.

B. Representative αSMA staining of mice from the indicated genotypes after chronic CCl_4 treatment.

C. Representative F4/80 staining of mice from the indicated genotypes after chronic CCl_4 treatment.

D. Representative flow cytometry of liver macrophages one day after chronic CCl_4 treatment. Percentages in the graph are of the gated population. Dot plot to the right of all performed experiments (n=5, each). Horizontal line represents the mean, each dot represents an experiment. Bars above each graph indicate standard error of the mean. **p<0.01, ***p<0.001.

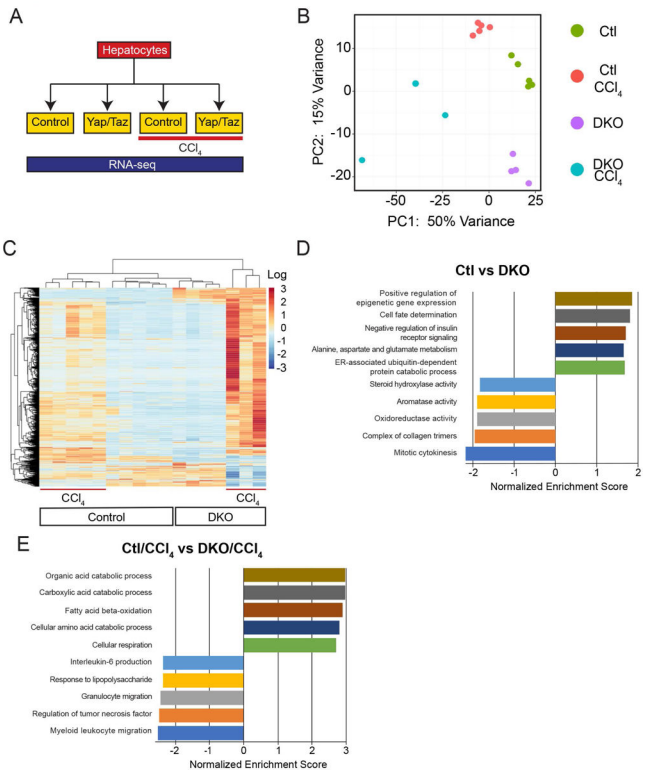

FIGURE 6. After Injury, YKO Hepatocytes Express More Metabolic and Fewer Immune Cell Migratory Programs than Controls

A. Treatment strategy diagram to analyze hepatocytes by RNA-seq.

B. Principal component analysis (PCA) of the indicated treatments.

C. Heat map of 1749 differentially expressed genes from the indicated treatments.

D. Top and bottom differentially expressed gene programs identified by GSEA for Ctl vs DKO.

E. Top and bottom differentially expressed gene programs identified by GSEA for Ctl/CCl_4 vs DKO/CCl_4

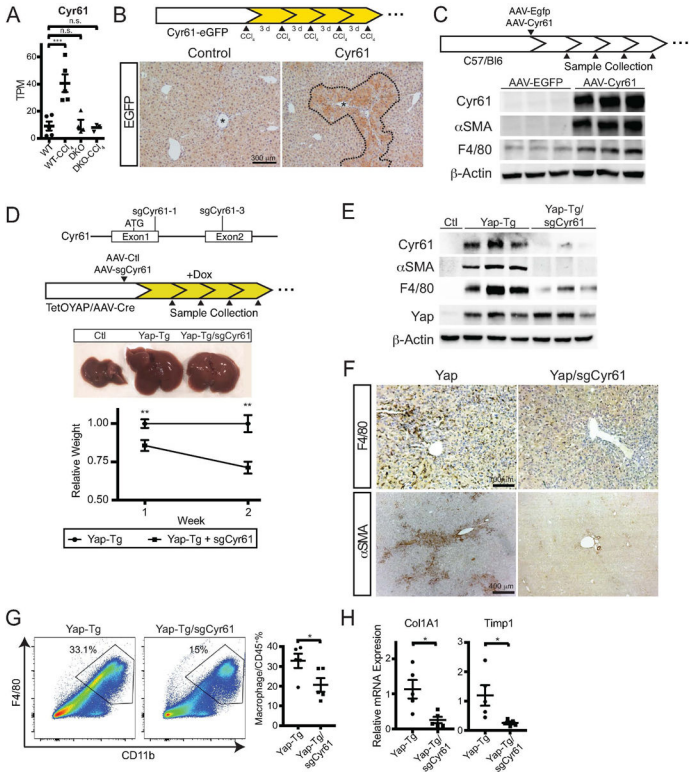

FIGURE 7. Cyr61 is the Primary Macrophage Chemoattractant Target of the Hippo Pathway

A. Cyr61 mRNA hepatocyte expression under the indicated conditions. Transcripts per million base pairs (TPM).

B. Representative EGFP staining of control and Cyr61-EGFP reporter mouse after chronic CCl_4 treatment. Asterisk marks central vein. Dotted line indicates area of $EGFP^+$ cells.

C. Strategy for either EGFP or Cyr61 expression in hepatocytes using AAV-TBG-EGFP or AAV-TBG-Cyr61. Below are whole-liver immunoblots of Cyr61, αSMA, F4/80, and β-actin for the indicated treatments one week after infection.

D. Strategy for Cyr61 deletion utilizing AAV-TBG-saCas9/Cyr61 sgRNAs delivered to TetOYAP mice with AAV-Cre. Middle: Gross pictures of Control, YAP-Tg, and YAP-Tg/sgCyr61 livers two weeks after YAP induction. Lower: Graph of relative weight between YAP-Tg and YAP-Tg/sgCyr61 livers at the indicated times (1 week, n=6/group; 2 week, n=5/group).

E. Immunoblots of control, YAP-Tg, YAP-Tg/sgCyr61 whole livers for Cyr61, αSMA, F4/80, YAP, and β-actin after 2 weeks of TetOYAP induction.

F. Representative immunostaining of YAP-Tg and YAP-Tg/sgCyr61 mice for F4/80 and αSMA after 2 weeks of TetOYAP induction.

G. Representative flow cytometry of liver macrophages in YAP-Tg and YAP-Tg/sgCyr61 liver after 2 weeks TetOYAP induction. Percentages shown are of gated population. Dot plot to the right of all performed experiments (n= 5, each). Horizontal line represents the mean, each dot represents and experiment. Bars above each graph indicate standard error of the mean.

H. Dot plots of Col1A1 and Timp1 expression by RT-qPCR from YAP-Tg and Yap-Tg/sgCyr61 whole livers at 2 weeks after TetOYAP induction. *p<0.05, **p<0.01, ***p<0.001

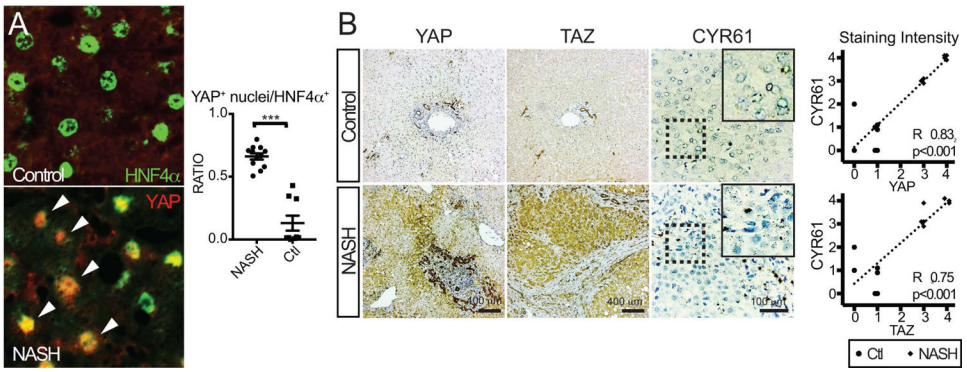

FIGURE 8. High Clinical NASH Activity Scores are Directly Associated with YAP/TAZ/CYR61 Expression

A. Immunostaining of representative human livers with low and high NASH activity for YAP and HNF4α. Right, dot plot quantification of each patient for YAP^+ nuclei/$HNF4\alpha^+$. Arrowheads indicate double positive cells.

B. Immunostaining (YAP, TAZ) or RISH (CYR61) of a cohort of human livers with low and high NASH activity (n=10, each) showing representative staining for each group. Graphs to the right show the relationship of YAP or TAZ immunostaining of each subject with respect to CYR61 expression. ***p<0.001